IOP Publishing — Journal of Physics D: Applied Physics
J. Phys. D: Appl. Phys. **40** (2007) 3461–3467 doi:10.1088/0022-3727/40/11/030

Evaluation of the chemical, electronic and optoelectronic properties of γ-CuCl thin films and their fabrication on Si substrates

F O Lucas[1,6], A Mitra[1], P J McNally[1], S Daniels[1], A L Bradley[2], D M Taylor[3], Y Y Proskuryakov[4], K Durose[4] and D C Cameron[5]

[1] Nanomaterials Processing Laboratory, Research Institute for Networks & Communications Engineering (RINCE), School of Electronic Engineering, Dublin City University, Dublin 9, Ireland
[2] Semiconductor Photonics Group, Physics Department, Trinity College, Dublin 2, Ireland
[3] Polymer Electronics Research Group, School of Electronic Engineering, University of Wales, Bangor, Gwynedd, LL57 1UT, UK
[4] Durham Centre for Renewable Energy, Department of Physics, Durham University, South Road, Durham, DH1 3LE, UK
[5] Advanced Surface Technology Research Laboratory (ASTRaL), Lappeenranta University of Technology, PO Box 181, Mikkeli 50101, Finland

E-mail: olalucas@eeng.dcu.ie and francis.lucas2@mail.dcu.ie

Received 6 March 2007, in final form 5 April 2007
Published 18 May 2007
Online at stacks.iop.org/JPhysD/40/3461

Abstract
CuCl is a I–VII semiconductor material with a direct band gap of ~3.4 eV. It exhibits a zincblende structure (γ-phase) at low temperatures, up to ~680 K. Unlike GaN, ZnO and related materials, CuCl has a relatively low lattice mismatch with Si (<0.4%) and a large excitonic binding energy (~190 meV). This suggests the possibility of the fabrication of excitonic-based blue/UV optoelectronic devices on Si with relatively low threading dislocation densities. In this study, CuCl has been deposited and examined as a candidate material for the fabrication of these devices. X-ray diffraction (XRD) measurements confirmed that the deposited films were preferentially oriented in the (1 1 1) plane. Room temperature photoluminescence measurements reveal a strong Z_3 free exciton peak (3.232 eV). Both steady state dc and ac impedance spectroscopy experiments suggested that the deposited CuCl is a mixed ionic–electronic semiconductor material. An electronic conductivity of the order of 2.3×10^{-7} S cm^{-1} was deduced to be in coexistence with Cu^+ ionic conductivity using irreversible electrodes (Au), while a total conductivity of the order of 6.5×10^{-7} S cm^{-1} was obtained using reversible electrodes (Cu) at room temperature. Further to this, we have identified some of the challenges in fabricating an optoelectronic device based on a CuCl/Si hybrid platform and propose some possible solutions.

(Some figures in this article are in colour only in the electronic version)

1. Introduction

In recent years, direct wide band gap semiconductor materials have been studied extensively by many researchers, due to their excellent thermal, optical and electrical properties. They have found applications in the manufacture of blue/UV light emitting diodes (LEDs), laser diodes, solar blind UV detectors, solar cells, gas sensors, high electron mobility transistors (HEMTs) and heterojunction bipolar transistors (HJTs) [1–3]. Since the commercialization of GaN-based LEDs [4] and laser

[6] Author to whom any correspondence should be addressed.

diodes [5] about ten years ago, gallium nitride and its related alloys have since then dominated the blue/UV optoelectronics industry. GaN is hexagonal (wurtzite) in structure, possessing a band gap of ∼3.43 eV and an excitonic binding energy of 23 meV [6]. In spite of the interesting thermal, optical and electrical performance of this material, devices produced from GaN suffer from numerous threading dislocations, due to the lack of an appropriate substrate. For instance the heteroepitaxy of GaN on sapphire (α-Al_2O_3) has a mismatch as high as 16% [7]. The introduction of epitaxial lateral overgrowth (ELOG) [8] and pendeoepitaxy techniques [9] for the deposition of GaN thin films has partially alleviated the problems of threading dislocations. Also the deposition of GaN on hexagonal silicon carbide (4H–SiC and 6H–SiC), with a lattice mismatch of ∼3.4% [10] has paved the way for the fabrication of GaN/SiC films with lower threading dislocation densities. However, these techniques are not straightforward especially in the latter case where Ga has poor wetting on the SiC surface [11]. In addition, the direct integration of GaN-based optoelectronics with Si microelectronics has been very difficult due to a lattice mismatch of ∼17%, thermal expansion coefficient incompatibility of ∼56% and the poor nucleation of GaN on Si [12].

ZnO, another promising material for the fabrication of blue/UV light emitting devices, has some advantages over GaN. These include an excitonic binding energy of 60 meV and the availability of high quality bulk single crystal. However, ZnO is usually deposited naturally as an n-type semiconductor material due to non-stoichiometry caused by zinc interstitials, oxygen vacancies or the incorporation of hydrogen in the crystal lattice [13–15]. Owing to self-compensation of charges, it is very difficult to prepare high quality p-type ZnO material reproducibly. The majority of the p-type ZnO films are usually characterized by a relatively low hole concentration, low hole mobility and instability [16–20], and the resulting p-type semiconductor may even appear to be n-type under the influence of ultraviolet photoelectron illumination [21]. As in the case for GaN, ZnO thin films face huge lattice mismatch problems with non-parental substrates and the difficulty of direct integration with well-stabilized Si microelectronics-based systems.

With a view of resolving these problems, we are currently investigating a new material system based on Copper I Chloride (CuCl) on Si. The large excitonic binding energy of ∼190 meV [22, 23] in CuCl guarantees the observation of excitonic recombination even up to room temperature and beyond [24]. In a similar fashion to ZnO but as opposed to GaN, high quality bulk single crystal CuCl can easily be grown. CuCl has been previously identified and recognized as a candidate material for the manufacture of electrooptic modulators and optical filters [25], as an electrolyte for solid-sate batteries [26], as a superconductor [27], as a photo-catalyst [28], in photography processing [29] and most recently as a sensor to detect CO in hydrogen environments [30]. In this study we have deposited and evaluated CuCl thin films for their chemical, electronic and optoelectronics properties and analysed the possibility of using a CuCl/Si hybrid platform for next generation optoelectronic devices.

2. Experimental

2.1. Film deposition

CuCl thin films of ∼0.5 μm thickness were grown by physical vapour deposition using an Edwards A306 vacuum evaporator at a base pressure of $\sim 1 \times 10^{-6}$ mbar. High purity commercially supplied CuCl with 99.999% purity (Alfa-Aesar) was evaporated from a quartz crucible at an approximately fixed deposition rate of 0.5 nm s^{-1} as indicted by the thickness monitor. The thin films of CuCl were deposited on cleaned square cut Si (1 0 0) substrates. The substrates were not externally heated during the evaporation process. Prior to deposition the substrates were ultrasonically cleaned with Decon Neutral® solution, organic solvents and deionized water. In addition to this conventional degreasing routine, the native oxide on the Si substrates was removed using hydrofluoric acid solution. Electrical contacts were made to the films by depositing copper and gold using vacuum evaporation or sputtering.

2.2. Characterization techniques

The phase purity and preferred orientation of the crystals at room temperature were examined on a Bruker AXS D8 advance x-ray diffractometer, using monochromatic Cu k_α radiation (λ = 0.154 nm). The surface morphology of the films was observed on a Nikon Eclipse ME6OOL optical microscope and a Digital Instruments Nanoscope III atomic force microscope (AFM). Semiquantitative chemical microanalysis and impurity detection was performed on a LEO Stereoscan 440 scanning electron microscope and a Princeton Gamma Tech energy dispersive x-ray analyser with a Si(Li) detector.

Optical measurements were taken using photoluminescence (PL) spectroscopy. Temperature-dependent PL measurements were carried out from room temperature down to 10 K by employing a UV Ar ion Innova laser with a second harmonic generation BBO crystal producing a 244 nm photoexcitation. The PL spectra were collected on a Jobin Yvon-Horiba Triax 190 spectrometer with a spectral resolution of 0.3 nm, coupled with a liquid nitrogen-cooled CCD detector.

Electrical characteristics were measured using both reversible and irreversible electrodes (copper and gold) in two configurations: Cu/CuCl/Cu and Au/CuCl/Au. Several structures were investigated including point planar, rectangular planar and sandwich electrode structures. Conventional lithography masking was used in defining these structures. Parasitic effects were excluded from the active area by the use of protective guards around the active region in a similar fashion to that in the work of Meijer *et al* [31]. Temperature-dependent ac measurements were examined using electro-impedance spectroscopy from 160 up to 400 K. Impedance spectra were recorded with a frequency network analyser (Solatron 1260) in a frequency range between 10 mHz and 1.5 MHz with a signal amplitude of 20 mV. Two point steady state room temperature current–voltage characteristics were obtained by utilizing an HP 4140B pA meter/dc voltage source as the source while the current was monitored. Electrical contacts were made to the electrodes by using a Cu or an

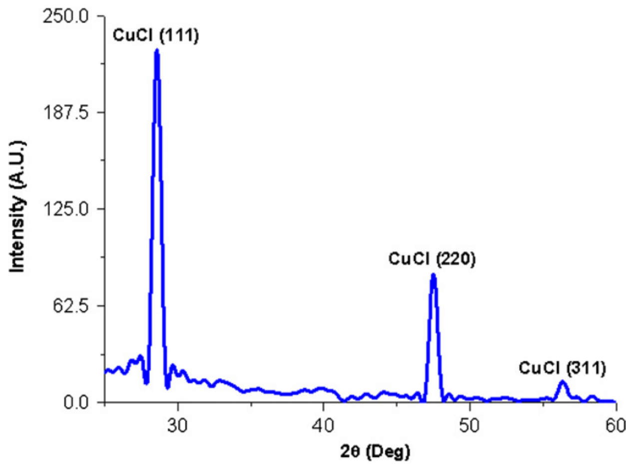

Figure 1. θ–2θ XRD pattern of CuCl film deposited on the Si (1 0 0) substrate.

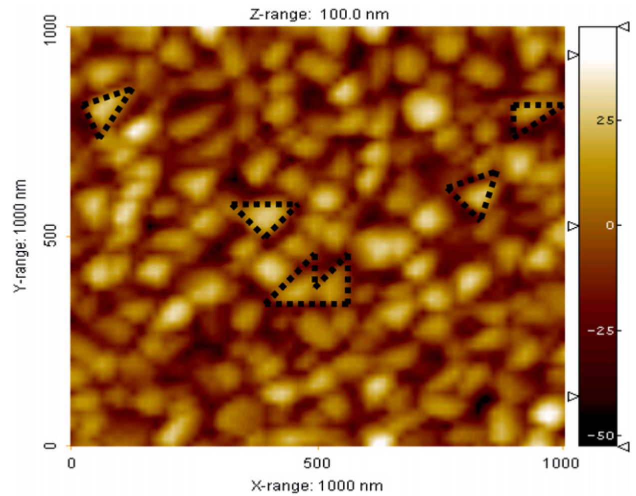

Figure 2. A typical AFM topograph of a 500 nm thick CuCl film deposited on the Si (1 0 0) substrate. Some of the triangular crystallites are highlighted by dotted triangles.

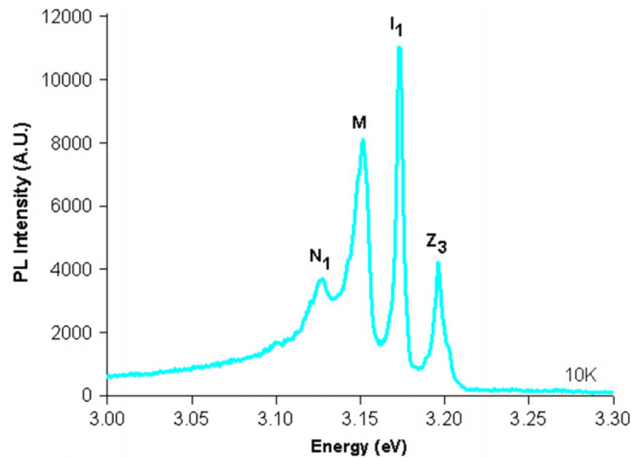

Figure 3. PL spectra of a 500 nm thick CuCl film deposited on the Si (1 0 0) substrate at 10 K.

Au jumper wire of 0.025 mm diameter (Advent Research Materials Ltd) and quick drying silver paint (Agar Scientific). The samples were mounted in a light-tight, earthed, steel vacuum chamber, allowing electrical characterizations at a base pressure of the order of 10^{-3} mbar.

3. Results and discussion

3.1. Structure, chemical analysis and morphology

The crystalline nature and structural parameters of the deposited CuCl films were identified by the XRD analysis. The presence of well-defined Bragg peaks (see figure 1) reveals the polycrystalline nature of the films and the 2θ values of these peaks are in excellent agreement with that of the ICDD powder diffraction database. The peaks centred around 28.5°, 47.5° and 56.4° correspond to the (1 1 1), (2 2 0) and (3 1 1) reflections, respectively. These are characteristic of γ-CuCl in the zincblende configuration. The XRD pattern of figure 1 also indicates that the (1 1 1) plane is the preferred orientation, which is also in good agreement with previous measurements of CuCl films on (0 0 0 1) Al_2O_3 [32]. An EDX microanalysis of the films confirmed the approximate stoichiometry of the CuCl compound and no major impurity contamination was identified. An example of a contact mode atomic force microscopy (AFM) measurement on the CuCl/Si films is shown in figure 2. This reveals some triangular crystallite features similarly to the previously reported MBE-grown CuCl films on (0 0 1) MgO [33]. Based on our experience with the deposition of CuCl films and the observation of Yanase *et al* [33], CuCl crystallises naturally in the (1 1 1) orientation and this tends to result in a triangular ⟨1 1 1⟩ oriented faceting on the growth substrate. The root mean square (RMS) roughness of the film was evaluated from the analysis of the AFM data to be 8.83 nm.

3.2. Optical properties

A typical low temperature PL spectrum at 10 K reveals four main peaks according to figure 3. The peak occurring at 3.204 eV is the familiar Z_3 free exciton. The peak located at 3.181 eV is the I_1 impurity bound exciton, a Cu vacancy having been suggested to be the impurity responsible for this emission [34]. The energy values of the Z_3 free exciton and the I_1 impurity bound exciton in this study are in excellent agreement with previous bulk CuCl crystal measurements [35]. The peak occurring at 3.160 eV is ascribed to the well-known free biexciton M [36], which originates from exciton–exciton collisions. Finally, the fourth peak centred at 3.135 eV is attributed to the N_1 impurity bound biexciton. The value of 3.135 eV is close to previous measurements on bulk crystals [37]. The temperature dependence of the PL spectra of CuCl/Si films is depicted in figure 4. The peak intensities of the impurity bound exciton I_1 and the impurity bound to biexciton N_1 decrease more rapidly in comparison with the free exciton Z_3 as the temperature increases. At temperatures above 80 K up to room temperature, the spectra are dominated by the Z_3 free exciton peak. The dominance and the stability of the Z_3 excitonic peak even up to room temperature is due to its large excitonic binding energy of the order of 190 meV. The temperature dependence of the Z_3 free exciton peak is seen in

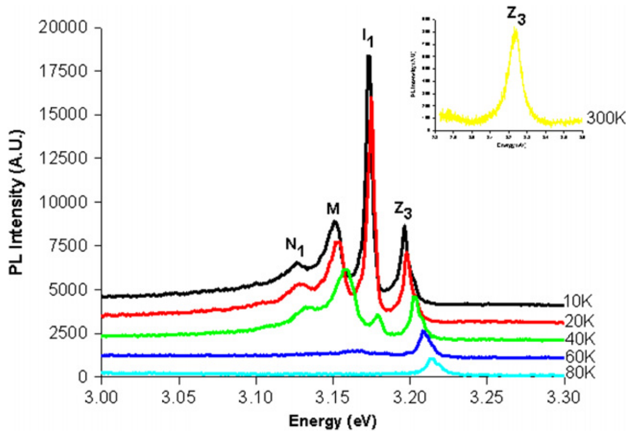

Figure 4. Temperature dependence of the PL spectrum of the CuCl film shown in figure 3.

figure 4 as the peak energy increases from 3.204 eV at 10 K to 3.232 eV at room temperature, which in turn indicates an increase in the band gap as the CuCl film warms up. The increase in the band gap energy as a function of temperature, which is in contrast to most semiconductors, was recently explained by Garro *et al* [38]. This anomalous effect is believed to be related to electron–phonon renormalization of the electronic structure of CuCl. They based their analysis on the fact that the Cu^{+} ions vibrating predominantly at low frequencies led to an increase in the band gap, whereas the Cl^{-} ions vibrating at high frequencies led to a reduction in the gap. The effect of the Cu^{+} ions becomes dominant as temperatures increase, which in turn results in an increase of the band gap energy as a function of temperature. Similar results have been previously reported for both thin films and nanocrystals of CuCl [39, 40].

3.3. Electrical properties

Steady state dc measurements. The current–voltage (I–V) characteristics of mixed conducting semiconductor materials can be greatly dependent on the type of electrode used [41]. In this study both reversible (Cu) and irreversible electrodes (Au) were employed, the difference being that Cu^{+} ions can swiftly be replaced with Cu but Au on the other hand, which is a blocking electrode, cannot do this. A typical I–V characteristic of Au/CuCl/Au structure at room temperature is shown in figure 5. The non-Ohmic response of the electrical characteristics is considered to be due to the bulk properties of CuCl and not interfacial effects. CuCl is a well-known mixed ionic–electronic semiconductor with p-type conductivity [42,43]. Following from general suggestions by Hebb [44], theoretical analysis [41] and experimental verification by Wagner and Wagner [43], an exponential current–voltage relation can be expected for a p-type mixed conduction material if the ionic current is suppressed by using blocking electrode(s) (Au). The hole conductivity, σ_h, in coexistence with the ionic conductivity in a mixed ionic semiconductor material under steady state conditions can in principle be estimated from the vertical intercept of the plot of $\ln I$ versus E using equation (1) [41, 43]:

$$\ln I = \ln(\sigma_h RTA/(Fd)) + EF/RT, \qquad (1)$$

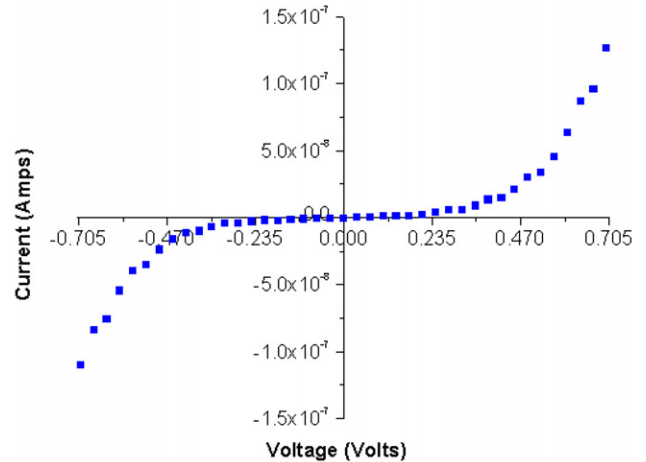

Figure 5. A typical room temperature I–V plot for a Au/CuCl/Au structure.

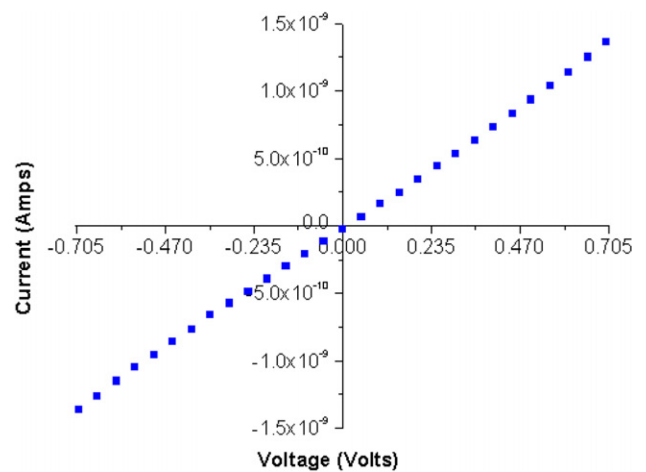

Figure 6. A typical room temperature I–V plot for a Cu/CuCl/Cu structure.

where R is the gas constant in J $\mathrm{Kmol^{-1}}$, T is the temperature in Kelvin, A is the active region area, F is Faraday's constant in C $\mathrm{mol^{-1}}$, d is the thickness of the sample and E is the steady state dc voltage which must be typically less than the decomposition voltage. A calculated hole conductivity of $\sim 2.3 \times 10^{-7}$ S $\mathrm{cm^{-1}}$ was deduced to be in coexistence with Cu^{+} ionic conductivity using equation (1). This value could be compared with a value of the order of 10^{-5} S $\mathrm{cm^{-1}}$ calculated for RF-sputtered CuBr films confined between gold electrodes [45]. The tendency corresponds to the increasing ionicity of bonds in the series: CuI $<$ CuBr $<$ CuCl.

With the films confined between Cu electrodes (figure 6), the same experiment gave an Ohmic relation with a maximum current density of about 100 times lower than that for the film with Au electrodes. This is not due to a contact limiting mechanism such as the well-known Schottky emission, but rather is in agreement with Wagner's defect chemistry analysis of mixed semiconducting materials [41]. Thus, when a mixed ionic–electronic material is equilibrated with its parental metal, it tends to become a nearly ideal stoichiometric material. This is due to the fact that excess Cu^{+} interstitial ions and Cu vacancies are consumed by the reversible nature of the Cu electrodes. A

total conductivity of 6.5×10^{-7} S cm^{-1} was obtained from the slope of the I–V data of figure 6, which is comparable to a value of the order of 10^{-8} S cm^{-1} obtained for bulk CuCl samples [46, 47].

Impedance spectroscopy (IS) measurement. IS is a powerful ac technique used in separating the bulk and interfacial phenomena in various materials [48]. The impedance data is often interpreted as a series of RC elements. The real (Z') and the imaginary (Z'') parts of the complex impedance are given by [49]

$$Z' = R_B/[1 + (\omega/\omega_B)^2] + R_{gb}/[1 + (\omega/\omega_{gb})^2] + R_{el}/[1 + (\omega/\omega_{el})^2] \quad (2)$$

and

$$Z'' = -[R_B(\omega/\omega_B)/[1 + (\omega/\omega_B)^2] + R_{gb}(\omega/\omega_{gb})/[1 + (\omega/\omega_{gb}) + R_{el}(\omega/\omega_{el})/[1 + (\omega/\omega_{el})^2]], \quad (3)$$

where subscripts B, gb and el represent the bulk, grain boundaries and electrode processes, respectively, and $\omega_i = 2\pi f_i = 1/(R_iC_i)$ is the angular frequency of the term i. The high frequency component of the complex impedance equation is normally ascribed to the bulk property as measured for single crystals [50], while the intermediate frequency and the low frequency terms correspond to the grain boundary and the electrode processes, respectively. In a situation where the grain boundaries and the electrode effects of the polycrystalline material are very small with respect to the bulk effect, equations (2) and (3) reduce to

$$Z' = R_B/[1 + (\omega/\omega_B)^2] = (R/[1 + (\omega RC)^2]), \quad (4)$$

$$Z'' = -R_B(\omega/\omega_B)/[1 + (\omega/\omega_B)^2] = -(\omega R^2C/[1 + (\omega RC)]^2). \quad (5)$$

The analysis of our impedance data was performed on a Nyquist plot ($-Z''$ versus Z'). Well-defined, single nearly ideal semicircles were obtained across the temperature range 160–400 K using Au electrodes. A typical example of such plots at 400 K is shown in figure 7 and thus equations (4) and (5) were employed to calculate the electrical parameters of the CuCl films. By examining figure 7, one can observe that the Nyquist plot has two solutions for the real impedance axis (Z') occurring at R_∞, as $\omega \to \infty$, and R_0, as $\omega \to 0$, and further to this, the quantity $|R_0 - R_\infty|$ is the resistance of the material. Using this simple analogy, the conductance of the CuCl films was obtained across the temperature range and fitted to the Arrhenius equation. The Arrhenius plot shows two distinct slopes, see figure 8. The activation energy above ~270 K was deduced to be 0.43 ± 0.01 eV, which is attributed to extrinsic Cu^+ ionic conduction by a vacancy mechanism and is in excellent agreement with previous works on compressed polycrystalline materials, 0.44 eV [47] and 0.45 eV [51]. By further examining figure 8, one notices a change in slope around 265 K whose activation energy varies slightly with different samples grown under the same experimental conditions. In all the cases, the activation energies of the samples were within a range of 40 ± 20 meV. At this temperature, the thermal activation energy is too low to maintain substantial ionic motion and thus the mode of conduction is ascribed to a dominant hole conduction mechanism. Similar activation energies for both Cu^+ ionic and hole conduction mechanisms have been demonstrated for CuBr, a closely related material [52, 53]. The difference in the values of the activation energy for different samples may be ascribed to the inability of the vacuum evaporation method to precisely deposit films with the same stoichiometry consistently. A similar variation of the electronic parameter was reported by Schmidt *et al* [54] for vacuum evaporated $NiMn_2O_{4+\delta}$ films.

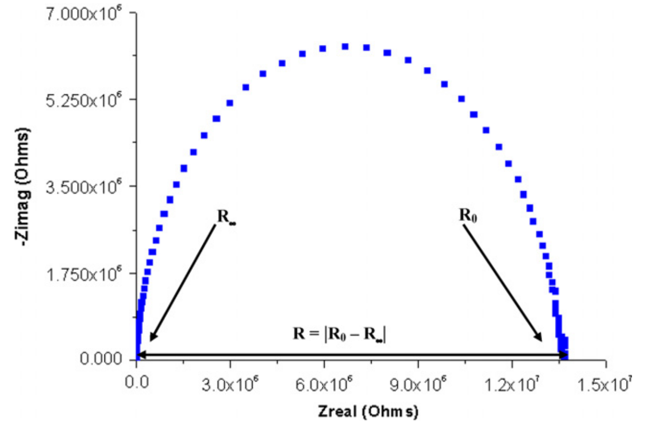

Figure 7. A Nyquist plot for the Au/CuCl/Au structure at 400 K.

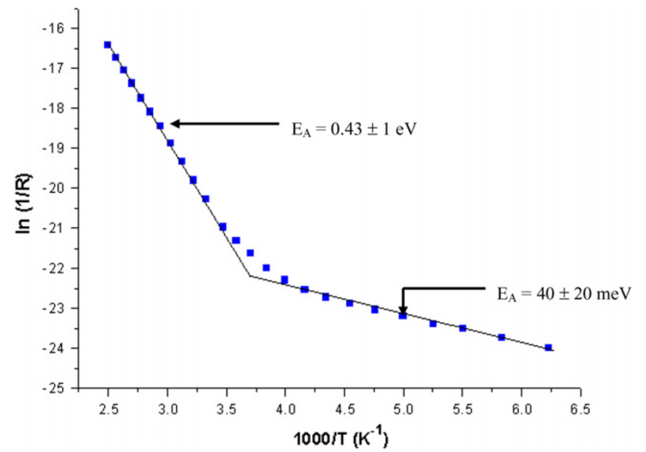

Figure 8. Arrhenius plot for the conductance of a typical CuCl film.

4. Electrolytic decomposition

Electrolytic decomposition otherwise known as electrolytic conduction is a well-known property of polar crystals, which has been established as far back as the 1920s. Tubandt and Eggert [55] in 1920 successfully demonstrated the transfer of Ag in silver iodide via an electrolytic conduction mechanism under the influence of a steady state source. Electrolytic decomposition is quite different from dielectric breakdown and occurs when a polar material is subjected to a steady state source greater than its decomposition threshold. According to [53], the threshold voltage is a function of the combination of the thermodynamic decomposition voltage, which could be deduced from the Gibbs free energy of formation of CuCl

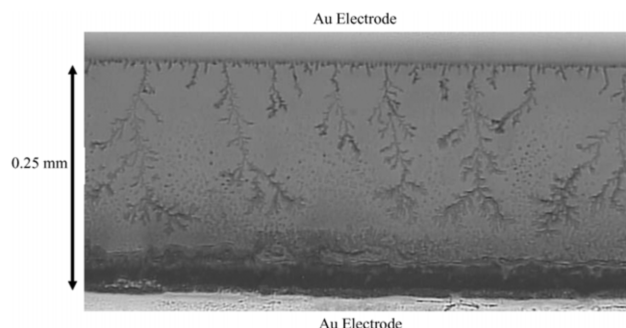

Figure 9. Optical micrograph of the electrolytic decomposition pattern of CuCl films.

(2CuCl → Cu + $CuCl_2$; 0.77 V and 2CuCl → 2Cu + Cl_2; 1.22 V at 298 K [56]), over voltages for different processes, including Ohmic drop, charge transfer at the electrodes (given by the Butler–Volmer equation [57]) and the nucleation of the electrodeposits. In our experiment, we have observed the onset of cathodic decomposition when a steady state voltage of more than 5 V was applied to CuCl films between a pair of rectangular planar Au electrodes with an inter electrode spacing of 0.25 mm. Figure 9 shows an example of such a Au/CuCl/Au structure subjected to 10 V steady state bias for 7 h. An EDX microanalysis on the fractal growth confirmed the dendrites are metallic copper.

5. Challenges

Like most semiconductor materials, CuCl presents its own challenges to achieving the primary goal of fabricating a Si compatible optoelectronic device. In the case of CuCl we have identified the following major challenges to resolve upon which we are currently working.

5.1. Thermal stability

The thermal stability of CuCl deposited on Si was earlier reported by O'Reilly *et al* [58]. It is believed that a reaction leading to the formation of $SiCl_4$ and Cu is formed by CuCl in contact with Si at temperatures above 523 K. For this reason devices fabricated from this hybrid platform must be dedicated to low–medium temperature range applications, typically less than 473 K.

5.2. Chemical stability

Cuprous halides are known to be very sensitive to air and moisture. CuCl as a member of this family oxidizes into oxy-halides of Cu II upon exposure to air [59]. We have initially demonstrated that thin films of CuCl could be encapsulated for a lengthy period greater than four weeks using organic polysilsesquioxane (PSSQ) and cyclo olefin copolymer (COC) encapsulants [60]. Most recently we have observed that the degradation of deposited CuCl films depends greatly on the purity of the source CuCl powder used for the evaporation and on the cleanliness of the substrate. Encapsulated films deposited from high purity freshly prepared CuCl powder upon very clean substrates have been found to be still chemically stable for a period greater than a year.

5.3. Electronic conductivity

It is well known that cuprous halides are mixed ionic–electronic semiconductor materials with a predominant Cu cationic conduction mechanism as previously explained. We are currently examining means of improving the electronic conductivity of CuCl films.

5.4. Electrolytic decomposition

This may be the greatest challenge in utilizing this material to fabricate optoelectronic devices. A thermodynamic decomposition voltage of 0.77 V was previously reported [55] for undoped CuCl. Such a low decomposition threshold voltage will obviously not favour any semiconductor device. In our experiments we have observed no decomposition when a steady state voltage of <5 V is applied to our CuCl films deposited as previously described. Despite the fact that no dendrites were observed on films subjected to a voltage of <5 V, this does not explicitly rule out the possibility of electrolytic decomposition. To this effect we are currently examining the stability of the fundamental electrical parameters (resistivity, carrier mobility, carrier density and carrier profiling) before and after being subjected to voltage stresses of up to 5 V.

6. Conclusion

In summary, CuCl has been deposited and assessed as a candidate material for the fabrication of Si compatible optoelectronic devices. Room temperature XRD results confirmed that the deposited CuCl films are zincblende in structure. PL measurements at 10 K reveal four main peaks ascribed to the Z_3 free exciton, I_1 impurity bound, M biexciton and the N_1 impurity bound exciton. Room temperature steady state dc measurements using reversible electrodes (Cu) gave an Ohmic response while using irreversible electrodes (Au) gave exponential I–V behaviour, both in conformance with Wagner's defect chemistry analysis of a mixed ionic–electronic material. The temperature dependence of the conductance of CuCl films deduced from impedance spectroscopy was interpreted as a change from extrinsic Cu^+ ionic conduction above 270 K to a hole conduction mechanism below that temperature, where the thermal energy is inadequate to maintain considerable ionic motion in the CuCl films. We are currently examining means of improving the low electronic conductivity and electrolytic decomposition problems of CuCl.

References

[1] Khan M A, Chen Q, Wang J W, Shur M S, Dermott B T and Higgins J A 1996 *IEEE Electron. Devices Lett.* **17** 325
[2] Tan S T, Chen B J, Sun X W, Hu X, Zhang X H and Chua S J 2005 *J. Cryst. Growth* **281** 571
[3] Xing H, McCarthy L, Keller S, DenBaars S P and Mishra U K 2000 *Proc. IEEE 27th Int. Symp. on Compound Semiconductors (Monterey, CA)* High current gain GaN bipolar junction transistors with regrown emitters p 365

[4] Nakamura S, Senoh M, Iwasa N, Nagahama S, Yamada T and Mukai T 1995 *Japan. J. Appl. Phys.* **34** L1332
[5] Nakamura S, Senoh M, Iwasa N, Nagahama S, Yamada T and Mutsushita T, Kiyoku H and Sugimoto Y 1996 *Japan. J. Appl. Phys.* **35** L74
[6] Vurgaftman I, Meyer J R and Ram-Mohan L R 2001 *J. Appl. Phys.* **89** 5815
[7] Kyeong J Jeong *et al* 2005 *J. Cryst. Growth* **276** 407
[8] Nakamura S *et al* 1998 *Appl. Phys. Lett.* **72** 211
[9] Davis R F, Gehrke T, Linthicum K J, Zheleva T S, Preble E A, Rajagopal P, Zorman C A and Mehregany M 2001 *J. Cryst. Growth* **225** 134
[10] Torvik J T, Qiu C, Leksono M and Pankove J I 1998 *Appl. Phys. Lett.* **72** 945
[11] Koleske D D, Henry R L, Twigg M E, Culbertson J C, Binari S C, Wickenden A E and Fatemi M 2002 *Appl. Phys. Lett.* **80** 4372
[12] Uen W, Li Z, Lan S and Liao S 2005 *J. Cryst. Growth* **280** 335
[13] Look D C, Hemsky J W and Sizelove J R 1999 *Phys. Rev. Lett.* **82** 2552
[14] Jung S, Kononenko V and Choi W 2006 *Solid State Commun.* **137** 474
[15] Pearton S J, Norton D P, Ip K, Heo Y W and Steiner T 2005 *Prog. Mater. Sci.* **50** 293
[16] Minegishi K, Koiwai Y, Kikuchi Y, Yano K, Kasuga M and Shimizu A 1997 *Japan. J. Appl. Phys.* **36** L1453
[17] Li X, Yan Y, Gessert T A, Dehart C, Perkins C L, Young D and Coutts T J 2003 *Electrochem. Solid State Lett.* **6** C56
[18] Guo H Tabata and Kawai T 2001 *J. Cryst. Growth* **223** 135
[19] Ashrafi A B M, Suemune I, Kumano H and Tanaka S 2002 *Japan. J. Appl Phys.* **41** L1281
[20] Barnes T M, Olson K and Wolden C A 2005 *Appl. Phys. Lett.* **86** 112112
[21] Perkins C L, Lee S-H, Li X, Asher S E and Coutts T J 2005 *J. Appl. Phys.* **97** 034907
[22] Grahn H T 1999 *Introduction to Semiconductor Physics* (Singapore: World Scientific)
[23] Ueta M, Kanzaki H, Kobayashi K, Toyosawa Y and Hanamura E 1986 *Excitonic Progresses in Solid* (Berlin: Springer)
[24] Reimann K and Rubenacke St 1994 *J. Appl. Phys.* **76** 4897
[25] Sterzer F, Blattner D and Miniter S 1964 *J. Opt. Soc. Am.* **54** 62
[26] Matsui T and Wagner J B Jr 1978 *Solid Electrolytes* ed P Hagemuller and W Van Gool (New York: Academic) p 237 and references therein
[27] Bardeen J 1978 *J. Less Comm. Met.* **62** 447
[28] Tennakone K, Punchihewa S and Tantrigoda R 1989 *Sol. Energy Mater.* **18** 217
[29] Reboul G 1911 *C. R. Hebd. Seances Acad. Sci.* **153** 1215
[30] Dutta P K, Rao R R, Swartz S L and Holt C T 2002 *Sensors Actuators* B **84** 189
[31] Meijer E J, Detchevery C, Baesjou P J, van Veenedaal E, de Leeuw D M and Klapwijk T M 2003 *J. Appl. Phys.* **93** 4831
[32] Nakayama M, Soumura A, Hamasaki K, Takeuchi H and Nishimura H 1997 *Phys. Rev.* B **55** 10099
[33] Yanase A and Segawa Y 1998 *Appl. Surf. Sci.* **130–132** 566
[34] Certier M, Wecker C and Nikitine S 1969 *J. Phys. Chem. Solids* **30** 2135
[35] Goto T, Takahashi T and Ueta M 1968 *J. Phys. Soc. Japan* **24** 314
[36] Nagasawa N, Nakata N, Doi Y and Ueta M 1975 *J. Phys. Soc. Japan* **39** 987
[37] Souma H, Goto T, Ohta T and Ueta M 1970 *J. Phys. Soc. Japan* **29** 697
[38] Garro N, Cantarero A, Cardona M, Ruf T, Göbel A, Lin C, Reimann K, Rtibenacke K and Steube M 1996 *Solid State Commun.* **98** 27
[39] Göbel A, Ruf T, Cardona M, Lin C T, Wrzesinski J, Steube M, Reimann K, Merle J-C and Joucla M 1998 *Phys. Rev.* B **57** 15183
[40] Pagés O, Erguig H, Lazreg A, Katty A, Lusson A and Gorochov O 2000 *Mater. Sci. Eng.* B **69–70** 431
[41] Wagner C 1956 *Z. Elektrochem.* **60** 4
[42] Joshi A V and Wagner J B Jr 1975 *J. Electrochem Soc.* **122** 1071
[43] Wagner J B and Wagner C 1957 *J. Chem. Phys.* **26** 1597
[44] Hebb M 1952 *J. Chem. Phys.* **20** 185
[45] Lauque P, Bendahan M, Seguin J-L, Pasquineli M and Knauth P 1999 *J. Eur. Ceram. Soc.* **19** 823
[46] Rivera J, Murray L A and Moss P A 1967 *J. Cryst. Growth* **1** 171
[47] Ida T, Saeki H, Hamada H and Kimura K 1996 *Surf. Rev. Lett.* **3** 41
[48] McDonald J R 1987 *Impedance Spectroscopy* (New York: Wiley)
[49] Abrantes J C C, Labrincha J A and Frade J R 2000 *Mater. Res. Bull.* **35** 727
[50] Denk I, Claus J and Maiser J 1997 *J. Electrochem. Soc.* **144** 3526
[51] Brune A and Wagner J B Jr 1995 *Mater. Res. Bull.* **30** 573
[52] Bendahan M, Seguin J-L, Lauque P, Aguir K and Knauth P 2003 *Sensors Actuators* B **95** 170
[53] Bendahan M, Jacolin C, Lauque P, Seguin J-L and Knauth P 2001 *J. Phys. Chem.* B **105** 8327
[54] Schmidt R, Basu A and Brinkman A W 2004 *J. Eur. Ceram. Soc.* **24** 1233
[55] Tubandt C and Eggert S 1920 *Z. f. Anorg. Chem.* **110** 196
[56] Harrison L G and Prasad M 1974 *J. Chem. Soc. Faraday Trans.* **I 70** 471
[57] Bard A and Faulkner L 1980 *Electrochemical Methods—Fundamentals and Applications* (New York: Wiley)
[58] O'Reilly L, Natarajan G, Lucas F O, McNally P J, Cameron D C, Reader A, Martinez-Rosas M and Bradley A L 2005 *J. Mater. Sci.: Electron. Mater.* **16** 415
[59] Schwab C and Goltzené A 1982 *Prog. Cryst. Growth Charact.* **5** 233
[60] Lucas F O *et al* 2006 *J. Cryst. Growth* **287** 112